pathways listed in Supplementary Table S9. Clustering analysis stratified the cell lines into 2 major groups, A and B (Supplementary Fig. S1). In comparison with group A, group B showed higher levels of phosphorylated MAPK signaling components including p-PDGF receptor-β(Thr751), p-Raf-A(Ser299) and phosphorylated signaling modules of the JNK and p38 MAPK pathways (Supplementary Fig S1, C1). Among them, the levels of p-p53 at Ser392, Ser37 and Ser6 differed substantially between groups A (low) and B (high) (Supplementary Fig. S1). In addition, cell lines clustered into group A tended to have simultaneous phosphorylation of the mTOR signaling components C2, S6RP(Ser235/236), S6RP(Ser240/244) and eIF4G(Ser1108) (Supplementary Fig S1). With some notable exceptions, sorafenib-insensitive cell lines (high IC50 values for sorafenib) and sorafenib-sensitive cell lines (low IC50 values for sorafenib) were clustered into group A and group B, respectively. Although sorafenib-insensitive SNU-387, JHH-1 and KIM-1 cells were classified into the sorafenib-sensitive group B, their phosphorylation levels of mTOR signaling component C2 were higher than those in the other cell lines in group B, suggesting that activation of mTOR signaling may be responsible for the resistance to sorafenib in these cell lines. Some of the sorafenib-insensitive cell lines (e.g., Alexander, JHH-2 and SNU-475 cells) partitioned into subtype Ab (Supplementary Fig. S1) were characterized by prominent activation of mTOR signaling component C2 and MAPK signaling component C1. Together, these findings imply that there is a certain population of HCC cells

showing up-regulation of both mTOR and MAPK signaling. Such a HCC subtype might respond better to combination treatment with mTOR and MAPK inhibitors. When we compared the phosphorylation status of the mTOR and MAPK signaling nodes in 95 cell lines by unsupervised hierarchical clustering, HCC cell lines were significantly clustered together ($p$ = 0.011 by Fisher's exact test) in group A (Supplementary Fig S2), characterized by high levels of phosphorylation of the signaling components C1 and C2, in comparison to cell lines derived from seven other cancer types (Supplementary Table 10). The signaling component C1 included previously reported targets of sorafenib such as b-RAF and PDGF receptor-β, as well as the upstream modules of the mTOR pathway (e.g., Akt and PDK). The component C2 comprised S6RP(Ser235/236), S6RP(Ser240/244) and eIF4G(Ser1108), and the signaling modules of the JNK and p38 MAPK pathways. These observations may reflect the fact that activation of MAPK signaling by itself, or in combination with mTOR signaling, is a unique feature of HCC.

It is noteworthy that some sorafenib-sensitive and insensitive cell lines were clustered together into subgroup Aa in Supplementary Fig. S1. Although this subgroup was characterized by relatively low levels of both mTOR and MAPK signaling activation, the most sorafenib-sensitive cell line, SNU-449, was classified into this subgroup. It is therefore plausible that some other signaling pathway, in addition to the mTOR and MAPK pathways, may be involved in defining the marked sensitivity of SNU-449 cells to sorafenib.

## Discussion

Derangements in the phosphorylation of signaling molecules are hallmarks of cancers, and are often considered as targets of molecular therapies. By profiling the phosphorylation status of multiple signaling components, it is possible to derive important clues for understanding the pathogenesis and classification of cancers. In this study, a high level of p-RPS6 S235/236 was detected in sorafenib-resistant HCC cells. Consistent with this *in vitro* observation, such high expression of p-RPS6 S235/236 was detected in pretreatment biopsy specimens from HCC patients who had shown early radiographically evident disease progression after starting sorafenib therapy. The number of patient samples analyzed in this study was small and insufficient for providing conclusive evidence, but the present findings warrant future clinical studies to evaluate the significance of p-RPS6 S235/236 as a predictor of response to sorafenib. In order to ensure accurate validation of the utility of p-RPS6 S235/236 as a predictor in future studies, standardized guidelines of immunohistochemistry for detecting p-RPS6 (Ser235/236) need to be developed, including tissue preparation, fixation, staining methods, scoring system and the definition of a "positive" result.

p-RPS6 has been used as a molecular surrogate for mTOR activation. Villanueva *et al.*

(22) assessed 314 surgical specimens of HCC immunohistochemically using an anti-p-RPS6 S240/244 antibody. They detected p-RPS6 S240/244 in half of the cases examined, and positive staining was correlated with HCC recurrence (22). Although antibodies against p-RPS6 S235/236 and p-RPS6 S240/244 have been used equivalently in many studies to evaluate mTOR activation (22, 23), the phosphoryation of these serine residues were found to be differentially regulated (Fig. 2A). An earlier study demonstrated persistent phosphorylation of RPS6 S235/236 in cells derived from $S6K1^{-/-}/S6K2^{-/-}$ double-knockout mice, and it was concluded that this paradoxical phosphorylation was caused by MAPK signaling. A later study revealed that RSK (MAPK pathway) predominantly phosphorylated the serine 235 and 236 residues of RPS6, whereas S6K (mTOR pathway) broadly phosphorylated the serine 235, 236, 240, 244, and 247 residues. Therefore, use of an antibody against p-RPS6 S240/244 would seem more appropriate for specific detection of the mTOR pathway activation status (20). In the present study, however, we found that phosphorylation of the serine 235 and 236 residues of RPS6 reflected crosstalk between the mTOR and MAPK pathways (Fig. 3C) and served as a predictive biomarker of sorafenib sensitivity. Although RAF kinases (MAPK pathway) are one of the main molecular types targeted by sorafenib, intervention of active mTOR signaling in the MAPK pathway seems to be one of the molecular mechanisms responsible for resistance of HCC to sorafenib.

It is therefore conceivable that HCC patients with tumors having high levels of p-RPS6 S235/236

could benefit from inhibition of mTOR signaling. We found that mTOR inhibitors showed higher anti-tumor activity against sorafenib-resisntant HCC cells (Fig. 3E). A recent phase I/II study of everolimus given daily as a single agent in patients with advanced HCC showed that the drug was well tolerated and exerted preliminary antitumor activity in some patients (24). A phase III EVOLVE-1 randomized trial is now ongoing to evaluate the efficacy of everolimus in HCC patients whose disease progressed during or after sorafenib treatment or who were intolerant to sorafenib (25). This clinical trial is designed to reveal the efficacy of mTOR pathway inhibition for control of sorafenib-resistant HCC, and is expected to clarify the significance of our present findings.

Clustering analysis of RPPA data revealed that 6 out of 23 HCC cell lines (Alexander, JHH-2, SNU-475, Huh-7, KIM-1 and JHH-1) had prominent activation of both the MAPK and mTOR pathways, indicating a possible subset of HCC patients who may benefit from a combination of MAPK and mTOR inhibitors (Supplementary Fig.S1). We also found synergy between MAPK and mTOR pathway inhibitors in sorafenib-resistant cell lines (Fig. 4). However, there is a need for caution before this can be applied clinically. Activation of MAPK signaling occurred at various levels of RAF/MEK/ERK/RSK in sorafenib-resistant cells (Fig. 3C). In addition, clustering analysis showed activation of two other major MAPK pathways, the Jun N-terminal kinase (JNK) and p38 MAPK pathways, in more than half the HCC cell lines

(Supplementary Fig.1). Cross-talk among three major MAPK pathways (RAF/MEK/ERK, JNK and p38MAPK) has been reported previously (26). Together, these findings suggest that careful assessment is vital when selecting an appropriate MAPK inhibitor for each individual HCC patient. Despite extensive sequencing of kinase genes, we were unable to identify any alterations in the pathway that might be responsible, indicating the need to expedite pharmacoproteomics for therapy personalization.

The present study highlighted the potential power of the RPPA platform for pathway profiling. We have provided proof-of-principle support for the utility of the highly sensitive, high-throughput RPPA platform by identifying a practical biomarker with potential clinical applicability. In this study, we used only well characterized antibodies with high specificity. The Human Antibody Initiative is an ongoing project to raise at least one monospecific antibody against all >20,000 proteins encoded by the human genome(27). It is anticipated that the completion of this project will greatly accelerate the capability of PRRP. The majority of current molecular targeting drugs are designed to target a particular signaling pathway (28). Precise determination of signaling pathways that are activated in individual patients seems to be essential for obtaining maximum benefit from any given treatment. RPPA requires only a minuscule specimen quantity (e.g., less than 1 ng protein per array) and is applicable even to small biopsy samples. The potential clinical utility of RPPA for decision-making and monitoring of cancer

therapeutics is thus enormous.

## References


1. Ferlay, J., Shin, H. R., Bray, F., Forman, D., Mathers, C., and Parkin, D. M. (2010) Estimates of worldwide burden of cancer in 2008: GLOBOCAN 2008. *Int J Cancer* 127, 2893-2917

2. Llovet, J. M., Ricci, S., Mazzaferro, V., Hilgard, P., Gane, E., Blanc, J. F., de Oliveira, A. C., Santoro, A., Raoul, J. L., Forner, A., Schwartz, M., Porta, C., Zeuzem, S., Bolondi, L., Greten, T. F., Galle, P. R., Seitz, J. F., Borbath, I., Haussinger, D., Giannaris, T., Shan, M., Moscovici, M., Voliotis, D., and Bruix, J. (2008) Sorafenib in advanced hepatocellular carcinoma. *N Engl J Med* 359, 378-390

3. Arao, T., Ueshima, K., Matsumoto, K., Nagai, T., Kimura, H., Hagiwara, S., Sakurai, T., Haji, S., Kanazawa, A., Hidaka, H., Iso, Y., Kubota, K., Shimada, M., Utsunomiya, T., Hirooka, M., Hiasa, Y., Toyoki, Y., Hakamada, K., Yasui, K., Kumada, T., Toyoda, H., Sato, S., Hisai, H., Kuzuya, T., Tsuchiya, K., Izumi, N., Arii, S., Nishio, K., and Kudo, M. (2013) FGF3/FGF4 amplification and multiple lung metastases in responders to sorafenib in hepatocellular carcinoma. *Hepatology* 57, 1407-1415

4. Cheng, A. L., Kang, Y. K., Chen, Z., Tsao, C. J., Qin, S., Kim, J. S., Luo, R., Feng, J., Ye, S., Yang, T. S., Xu, J., Sun, Y., Liang, H., Liu, J., Wang, J., Tak, W. Y., Pan, H., Burock, K., Zou, J., Voliotis, D., and Guan, Z. (2009) Efficacy and safety of sorafenib in patients in the Asia-Pacific region with advanced hepatocellular carcinoma: a phase III randomised, double-blind, placebo-controlled trial. *Lancet Oncol* 10, 25-34

5. Wilhelm, S. M., Adnane, L., Newell, P., Villanueva, A., Llovet, J. M., and Lynch, M. (2008) Preclinical overview of sorafenib, a multikinase inhibitor that targets both Raf and VEGF and PDGF receptor tyrosine kinase signaling. *Mol Cancer Ther* 7, 3129-3140

6. Abou-Alfa, G. K., Schwartz, L., Ricci, S., Amadori, D., Santoro, A., Figer, A., De Greve, J., Douillard, J. Y., Lathia, C., Schwartz, B., Taylor, I., Moscovici, M., and Saltz, L. B. (2006) Phase II study of sorafenib in patients with advanced hepatocellular carcinoma. *J Clin Oncol* 24, 4293-4300

7. Ueshima, K., Kudo, M., Takita, M., Nagai, T., Tatsumi, C., Ueda, T., Kitai, S., Ishikawa, E., Yada, N., Inoue, T., Hagiwara, S., Minami, Y., Chung, H., and Sakurai, T. (2011) Des-gamma-carboxyprothrombin may be a promising biomarker to determine the therapeutic efficacy of sorafenib for hepatocellular carcinoma. *Dig Dis* 29, 321-325

8. Hagiwara, S., Kudo, M., Nagai, T., Inoue, T., Ueshima, K., Nishida, N., Watanabe, T., and Sakurai, T. (2012) Activation of JNK and high expression level of CD133 predict a poor response to sorafenib in hepatocellular carcinoma. *Br J Cancer* 106, 1997-2003

9. Nishizuka, S., Charboneau, L., Young, L., Major, S., Reinhold, W. C., Waltham, M., Kouros-Mehr, H., Bussey, K. J., Lee, J. K., Espina, V., Munson, P. J., Petricoin, E., 3rd, Liotta, L. A., and Weinstein, J. N. (2003) Proteomic profiling of the NCI-60 cancer cell lines using new high-density reverse-phase lysate microarrays. *Proc Natl Acad Sci U S A* 100, 14229-14234

10. Byers, L. A., Wang, J., Nilsson, M. B., Fujimoto, J., Saintigny, P., Yordy, J., Giri, U., Peyton,

M., Fan, Y. H., Diao, L., Masrorpour, F., Shen, L., Liu, W., Duchemann, B., Tumula, P., Bhardwaj, V., Welsh, J., Weber, S., Glisson, B. S., Kalhor, N., Wistuba, II, Girard, L., Lippman, S. M., Mills, G. B., Coombes, K. R., Weinstein, J. N., Minna, J. D., and Heymach, J. V. (2012) Proteomic profiling identifies dysregulated pathways in small cell lung cancer and novel therapeutic targets including PARP1. *Cancer Discov* 2, 798-811

11. Spurrier, B., Ramalingam, S., and Nishizuka, S. (2008) Reverse-phase protein lysate microarrays for cell signaling analysis. *Nat Protoc* 3, 1796-1808

12. Bolstad, B. M., Irizarry, R. A., Astrand, M., and Speed, T. P. (2003) A comparison of normalization methods for high density oligonucleotide array data based on variance and bias. *Bioinformatics* 19, 185-193

13. Masuda, M., Maruyama, T., Ohta, T., Ito, A., Hayashi, T., Tsukasaki, K., Kamihira, S., Yamaoka, S., Hoshino, H., Yoshida, T., Watanabe, T., Stanbridge, E. J., and Murakami, Y. (2010) CADM1 interacts with Tiam1 and promotes invasive phenotype of human T-cell leukemia virus type I-transformed cells and adult T-cell leukemia cells. *J Biol Chem* 285, 15511-15522

14. Li, H., and Durbin, R. (2009) Fast and accurate short read alignment with Burrows-Wheeler transform. *Bioinformatics* 25, 1754-1760

15. Li, H., Handsaker, B., Wysoker, A., Fennell, T., Ruan, J., Homer, N., Marth, G., Abecasis, G., Durbin, R., and Genome Project Data Processing, S. (2009) The Sequence Alignment/Map format and SAMtools. *Bioinformatics* 25, 2078-2079

16. Wang, K., Li, M. Y., and Hakonarson, H. (2010) ANNOVAR: functional annotation of genetic variants from high-throughput sequencing data. *Nucleic Acids Research* 38

17. Chou, T. C. (2010) Drug combination studies and their synergy quantification using the Chou-Talalay method. *Cancer Res* 70, 440-446

18. Anjum, R., and Blenis, J. (2008) The RSK family of kinases: emerging roles in cellular signalling. *Nat Rev Mol Cell Biol* 9, 747-758

19. Pende, M., Um, S. H., Mieulet, V., Sticker, M., Goss, V. L., Mestan, J., Mueller, M., Fumagalli, S., Kozma, S. C., and Thomas, G. (2004) S6K1(-/-)/S6K2(-/-) mice exhibit perinatal lethality and rapamycin-sensitive 5'-terminal oligopyrimidine mRNA translation and reveal a mitogen-activated protein kinase-dependent S6 kinase pathway. *Mol Cell Biol* 24, 3112-3124

20. Roux, P. P., Shahbazian, D., Vu, H., Holz, M. K., Cohen, M. S., Taunton, J., Sonenberg, N., and Blenis, J. (2007) RAS/ERK signaling promotes site-specific ribosomal protein S6 phosphorylation via RSK and stimulates cap-dependent translation. *J Biol Chem* 282, 14056-14064

21. Ascierto, P. A., Kirkwood, J. M., Grob, J. J., Simeone, E., Grimaldi, A. M., Maio, M., Palmieri, G., Testori, A., Marincola, F. M., and Mozzillo, N. (2012) The role of BRAF V600 mutation in melanoma. *J Transl Med* 10, 85

22. Villanueva, A., Chiang, D. Y., Newell, P., Peix, J., Thung, S., Alsinet, C., Tovar, V., Roayaie, S., Minguez, B., Sole, M., Battiston, C., Van Laarhoven, S., Fiel, M. I., Di Feo, A., Hoshida, Y., Yea, S.,

Toffanin, S., Ramos, A., Martignetti, J. A., Mazzaferro, V., Bruix, J., Waxman, S., Schwartz, M., Meyerson, M., Friedman, S. L., and Llovet, J. M. (2008) Pivotal role of mTOR signaling in hepatocellular carcinoma. *Gastroenterology* 135, 1972-1983, 1983 e1971-1911

23. Zhou, L., Huang, Y., Li, J., and Wang, Z. (2010) The mTOR pathway is associated with the poor prognosis of human hepatocellular carcinoma. *Med Oncol* 27, 255-261

24. Zhu, A. X., Abrams, T. A., Miksad, R., Blaszkowsky, L. S., Meyerhardt, J. A., Zheng, H., Muzikansky, A., Clark, J. W., Kwak, E. L., Schrag, D., Jors, K. R., Fuchs, C. S., Iafrate, A. J., Borger, D. R., and Ryan, D. P. (2011) Phase 1/2 study of everolimus in advanced hepatocellular carcinoma. *Cancer* 117, 5094-5102

25. Kudo, M. (2011) Signaling pathway and molecular-targeted therapy for hepatocellular carcinoma. *Dig Dis* 29, 289-302

26. Wagner, E. F., and Nebreda, A. R. (2009) Signal integration by JNK and p38 MAPK pathways in cancer development. *Nat Rev Cancer* 9, 537-549

27. Uhlen, M., and Ponten, F. (2005) Antibody-based proteomics for human tissue profiling. *Molecular & cellular proteomics : MCP* 4, 384-393

28. Wulfkuhle, J. D., Edmiston, K. H., Liotta, L. A., and Petricoin, E. F., 3rd (2006) Technology insight: pharmacoproteomics for cancer--promises of patient-tailored medicine using protein microarrays. *Nat Clin Pract Oncol* 3, 256-268

## Figure Legends

**Figure 1. Phosphoprofiling of key signaling molecules by RPPA.**

**(A)** Phosphorylation status of 180 signaling nodes in a panel of 95 cancer cell lines cultured in the presence of 10% FCS. Red and blue colors indicate high- and low-level phosphorylation, respectively. **Abbreviations:** STAT, signal transducers and activators of transcription; SAPK/JNK, stress-activated protein kinase/c-Jun NH2-terminal kinase; RTK, receptor tyrosine kinase; PI3K, phosphatidylinositol 3'-kinase; MAPK, mitogen-activated protein kinase; NFκB, nuclear factor-kappaB; OS, osteosarcoma; OSCC, oral squamous cell carcinoma.

**(B)** Immunoblot (left) and RPPA (right) analyses of A431 cells cultured without (-) and with (+) EGF for 10 minutes with anti-p-ERK1/2 (T202/Y204) antibody. The mean fluorescence intensity in arbitrary units (top) and images (bottom) of quadruplicate RPPA spots of lysate undiluted (1) and diluted 1:2 (1/2), 1:4 (1/4), and 1:8 (1/8) -fold are shown (right).

**(C and D)** Relative p-RPS6 S235/236 (C) and p-Met T1234/1235 (D) expression of 95 cell lines determined by RPPA (right). Cell lines with the 3 highest and 3 lowest levels of expression were selected and subjected to immunoblotting with the same antibody (left). **Abbreviations:** Ave, average.

**Figure 2. p-RPS6 S235/236 correlates with the sensitivity of HCC to sorafenib.**

**(A)** Upper graph: IC50 values for sorafenib against 23 HCC cell lines sorted from the most sensitive (left) to resistant (right) ones. Columns and error bars represent the mean and SD of three independent experiments, respectively. Lower panels: Immunoblot analysis of pRPS6 S235/236, pRPS6 S240/244, RPS6, and γ-tubulin (loading control) expression in the 23 HCC cell lines.

**(B)** Correlation between RPPA and immunoblot analyses of p-RPS6 S235/236 expression in the 23 HCC cell lines ($R^2 = 0.733$).

**(C)** Detection of p-RPS6 S235/236 in pretreatment biopsy samples. Hematoxylin and eosin (H&E) (a-d1) and immunoperoxidase staining with anti-p-RPS6 S235/236 (a-d2) and total RPS6 (a-d3) antibodies of HCC biopsy specimens obtained from a responder [patient 1 (a and b)] and a representative non-responder [patient 2 (c and d)] to sorafenib. Original magnification was ×40 (a1-3 and c1-3) and ×200 (b1-3 and d1-3).

**Figure 3. Alternative mTOR signal activation in sorafenib-resistant HCC cells.**

**(A and C)** Representative sorafenib-sensitive (HUH-6 and HuH-7) and -resistant (JHH-1, JHH-2, SNU-182, SNU423, and SNU-387) HCC cells were treated with the indicated concentrations of sorafenib for 3 hours, and the expression of p-RPS6 S235/236, total RPS6, p-ERK1/2

T202/Y204, total ERK, p-RSK T380, total RSK, p-S6K T389, and total S6K was determined by immunoblotting.

**(B)** Schematic representation of the mTOR and MAPK pathways and their inhibitors.

**(D)** Representative sorafenib-resistant (JHH-1, JHH-2, SNU-182, SNU423, and SNU-387) HCC cells were treated with the indicated concentrations of everolimus for 3 hours, and the expression of p-RPS6 S235/236 and total RPS6 was determined by immunoblotting.

**(E)** Distribution of IC50 values of representative sorafenib-sensitive (SNU-449, HUH-6, JHH-7, HuH-7, and SK-Hep1) and -resistant (JHH-1, JHH-2, SNU-182, SNU-423, and SNU-387) HCC cells to AZ8055. Boxes indicate 25-75th percentiles.

**Figure 4. Synergy of mTOR and MAPK inhibitors.**

**(A)** Sorafenib-resistant JHH-1 and SNU-182 cells were treated with the indicated concentrations of sorafenib and everolimus, and the expression of p-RPS6 S235/236 and total RPS6 was examined by immunoblotting (top). The bottom panel indicates intensity relative to control blots (no treatment).

**(B)** Sorafenib-resistant JHH-1 and SNU-182 cells were treated with the indicated concentrations of CI-1040, SL0101, and everolimus, and the expression of p-RPS6 S235/236 and RPS6 was

examined by immunoblotting (top). The bottom panel indicates blot intensities relative to control blots (no drug treatment).

**(C)** Sorafenib-resistant SNU-423 cells were treated with the indicated concentrations of CI-1040, and relative cell viability was determined 72 hours later. Note that CI-1040 had no significant cell growth-inhibitory effect at 0.1 μM (indicated by a red arrow).

**(D)** Sorafenib-resistant SNU-423 cells were untreated (solid circles) or treated (clear circles) with 0.1 μM CI-1040 and the indicated concentrations of AZD8055, and relative cell viability was determined 72 hours later.

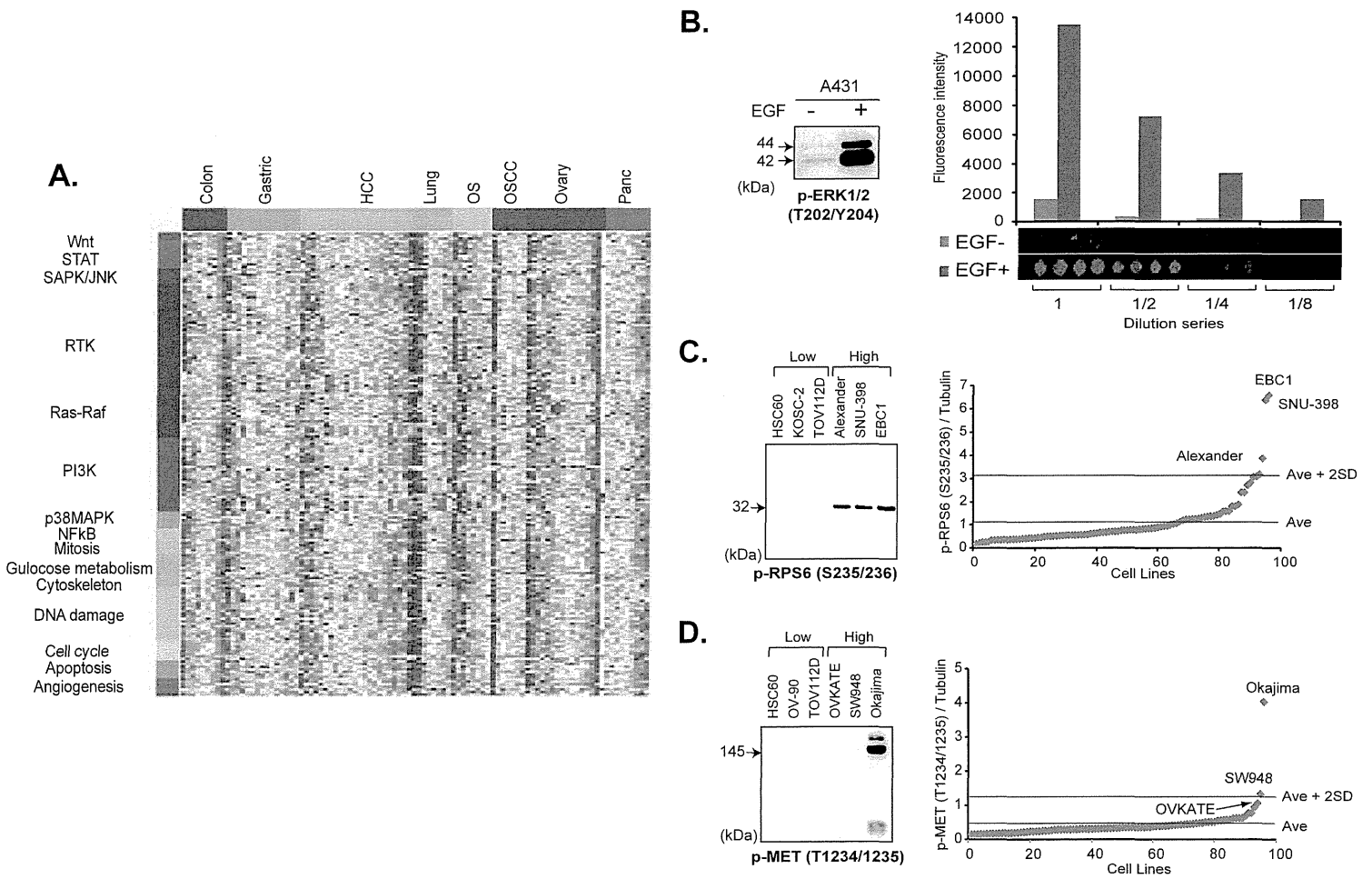

A.
Colon
Gastric
HCC
Lung
OS
OSCC
Ovary
Panc
Wnt
STAT
SAPK/JNK
RTK
Ras-Raf
PI3K
p38MAPK
NFkB
Mitosis
Gulocose metabolism
Cytoskeleton
DNA damage
Cell cycle
Apoptosis
Angiogenesis
B.
A431
EGF - +
44
42
(kDa)
p-ERK1/2
(T202/Y204)
Fluorescence intensity
14000
12000
10000
8000
6000
4000
2000
0
EGF-
EGF+
1
1/2
1/4
1/8
Dilution series
C.
Low
High
HSC60
KOSC-2
TOV112D
Alexander
SNU-398
EBC1
32
(kDa)
p-RPS6 (S235/236)
p-RPS6 (S235/236) / Tubulin
EBC1
SNU-398
Alexander
Ave + 2SD
Ave
Cell Lines
D.
Low
High
HSC60
OV-90
TOV112D
OVKATE
SW948
Okajima
145
(kDa)
p-MET (T1234/1235)
p-MET (T1234/1235) /Tubulin
Okajima
SW948
Ave + 2SD
OVKATE
Ave
Cell Lines

**Figure 1.**

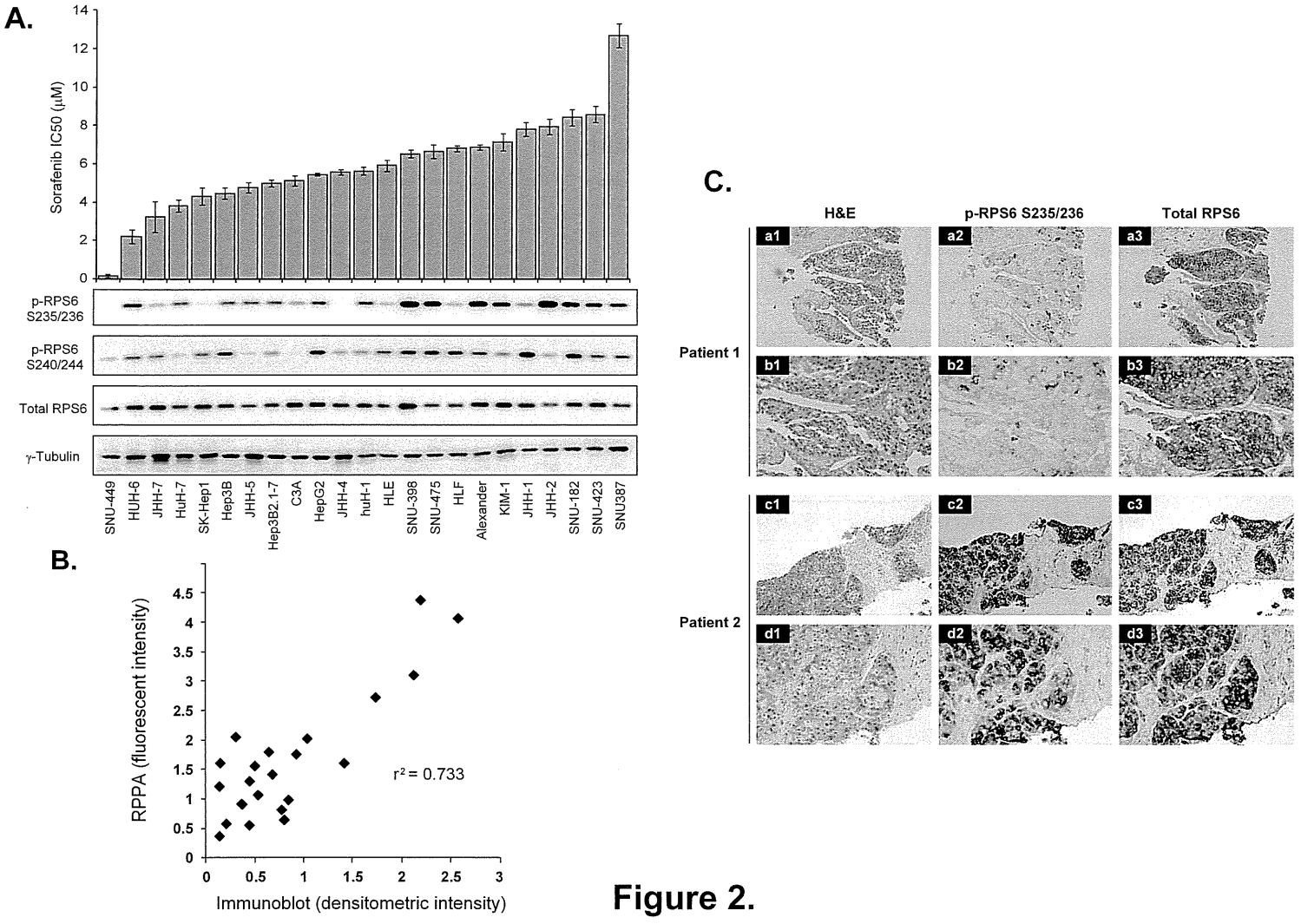

A.
Sorafenib IC50 (μM)
p-RPS6 S235/236
p-RPS6 S240/244
Total RPS6
γ-Tubulin
SNU-449
HUH-6
JHH-7
HuH-7
SK-Hep1
Hep3B
JHH-5
Hep3B2.1-7
C3A
HepG2
JHH-4
huH-1
HLE
SNU-398
SNU-475
HLF
Alexander
KIM-1
JHH-1
JHH-2
SNU-182
SNU-423
SNU387
B.
RPPA (fluorescent intensity)
Immunoblot (densitometric intensity)
r² = 0.733
C.
H&E
p-RPS6 S235/236
Total RPS6
Patient 1
Patient 2
a1
a2
a3
b1
b2
b3
c1
c2
c3
d1
d2
d3

**Figure 2.**

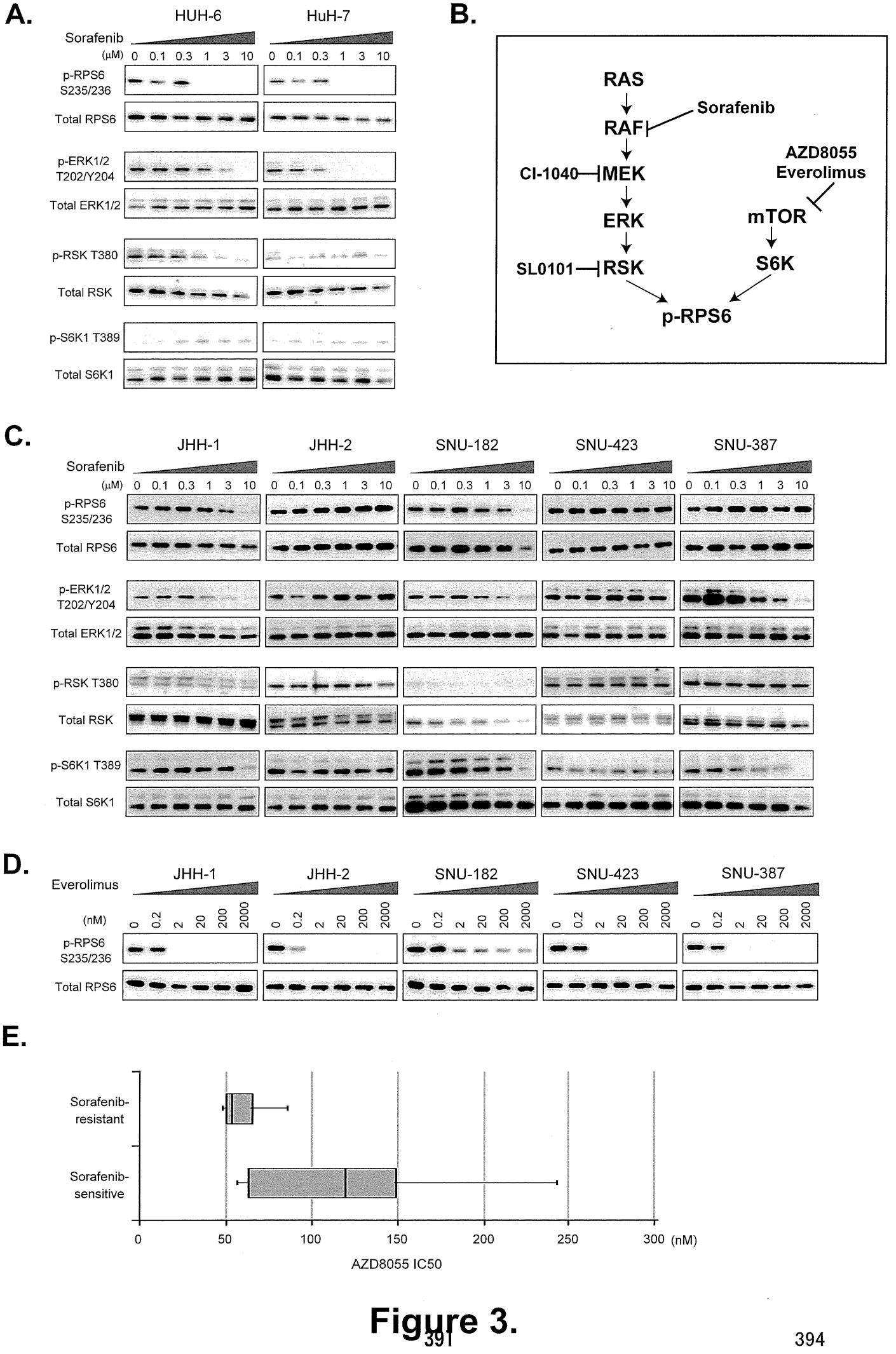

A.
HUH-6
HuH-7
Sorafenib
(μM) 0 0.1 0.3 1 3 10
p-RPS6 S235/236
Total RPS6
p-ERK1/2 T202/Y204
Total ERK1/2
p-RSK T380
Total RSK
p-S6K1 T389
Total S6K1
B.
RAS
RAF
Sorafenib
MEK
CI-1040
ERK
RSK
SL0101
AZD8055
Everolimus
mTOR
S6K
p-RPS6
C.
JHH-1
JHH-2
SNU-182
SNU-423
SNU-387
Sorafenib
(μM) 0 0.1 0.3 1 3 10
p-RPS6 S235/236
Total RPS6
p-ERK1/2 T202/Y204
Total ERK1/2
p-RSK T380
Total RSK
p-S6K1 T389
Total S6K1
D.
Everolimus
(nM) 0 0.2 2 20 200 2000
p-RPS6 S235/236
Total RPS6
E.
Sorafenib-resistant
Sorafenib-sensitive
0 50 100 150 200 250 300 (nM)
AZD8055 IC50

**Figure 3.**

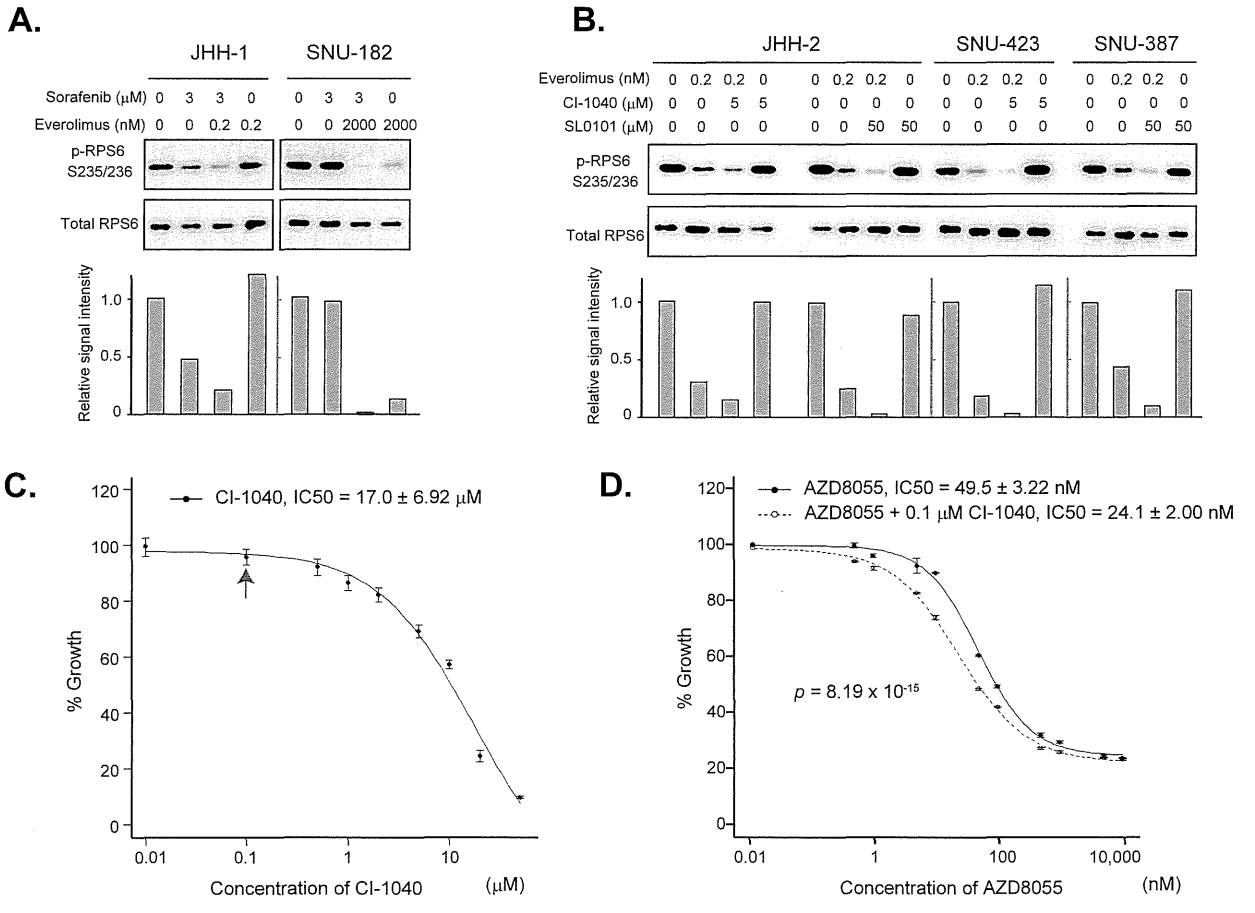

A.
JHH-1
SNU-182
Sorafenib (μM) 0 3 3 0 0 3 3 0
Everolimus (nM) 0 0 0.2 0.2 0 0 2000 2000
p-RPS6 S235/236
Total RPS6
Relative signal intensity
1.0
0.5
0
B.
JHH-2
SNU-423
SNU-387
Everolimus (nM) 0 0.2 0.2 0 0 0.2 0.2 0 0 0.2 0.2 0 0 0.2 0.2 0
CI-1040 (μM) 0 0 5 5 0 0 0 0 0 0 5 5 0 0 0 0
SL0101 (μM) 0 0 0 0 0 0 50 50 0 0 0 0 0 0 50 50
p-RPS6 S235/236
Total RPS6
Relative signal intensity
1.0
0.5
0
C.
CI-1040, IC50 = 17.0 ± 6.92 μM
% Growth
120
100
80
60
40
20
0
0.01
0.1
1
10
Concentration of CI-1040 (μM)
D.
AZD8055, IC50 = 49.5 ± 3.22 nM
AZD8055 + 0.1 μM CI-1040, IC50 = 24.1 ± 2.00 nM
p = 8.19 x 10-15
% Growth
120
100
80
60
40
20
0
0.01
1
100
10,000
Concentration of AZD8055 (nM)

**Figure 4.**

## Supplementary Figure Legends

**Figure S1. Unsupervised hierarchical clustering of the 23 HCC cell lines (horizontal axis) and phosphorylation status of the mTOR and MAPK signaling nodes (vertical axis).** Red, white and blue colors indicate high, intermediate and low levels of signaling node phophorylation. Light green and yellow represent signaling components of the MAPK pathway and mTOR pathway, respectively. Signaling components of the MAPK and mTOR pathways highly related to HCC cell line subtypes are labeled C1 and C2, respectively. Clustering revealed formation of 2 major groups, A and B, in the cell lines. The 10 cell lines that showed the highest IC50 for sorafenib are highlighted in orange.

**Figure S2. Unsupervised hierarchical clustering of the 95 HCC cell lines (horizontal axis) and phosphorylation status of the mTOR and MAPK signaling nodes (vertical axis).** Red, white and blue colors indicate high, intermediate and low levels of signaling node phophorylation. Light green and yellow represent signaling components of the MAPK pathway and mTOR pathway, respectively. Signaling components related to HCC cell line subtypes are labeled C1 and C2, respectively. Clustering revealed formation of 2 major groups, A and B, in the cell lines. The 23 HCC cell lines are highlighted in purple.

## LIST OF TABLES

**Supplementary Table S1.** List of cell lines used for RPPA construction.

**Supplementary Table S2.** List of 180 phosphorylation site-specific antibodies.

**Supplementary Table S3.** Correlation between sensitivity to sorafenib and the phosphorylation of 180 signaling molecules.

**Supplementary Table S4.** Clinical characteristics of patients.

**Supplementary Table S5.** List of the 511 kinase genes sequenced.

**Supplementary Table S6.** Kinase gene alterations in HCC cells.

**Supplementary Table S7.** mTOR and MAPK pathway gene alterations in HCC cells.

**Supplementary Table S8.** Chou-Talalay median dose effect analysis.

**Supplementary Table S9.** List of the MAPK and mTOR signaling components used for unsupervised hierarchical clustering analyses.

**Supplementary Table S10.** Fisher's exact test: Association of cancer types with activation status of MAPK and mTOR signaling.